

Modeling the Effect of the Stress Demagnetization Phenomenon on the Magnetic Properties in a NO Fe-Si 3% Sheet

Malika Yakhlef¹, Sebti Boukhtache¹, Mabrouk Chabane¹

Abstract: The aim of this paper is the modeling of the stress demagnetization effect on the magnetic properties in a non-oriented Fe-Si 3% sheet under different external stresses. The magneto-mechanical model used for magnetic hysteresis is based on a model originally formulated by Sablik-Jiles-Atherthon (S.J.A.). This latter has been modified by including both the stress demagnetization factor and the eddy current effects. The influence of the stress demagnetization term SDT on the magnetostrictive behavior of the material is also modeled. The proposed model has been validated by extensive simulations at different stresses, namely compressive and tensile stresses. Simulation results obtained by this model are very close to those published in the literature. Using the proposed model, very satisfactory performance has been achieved.

Keywords: Magneto-mechanical model, Stress demagnetization effect, Eddy current, Magnetic properties, Magnetostriction, NO Fe-Si 3% Sheets.

1 Nomenclature

- M – Total magnetization [A/m];
- M_S – Saturation magnetization [A/m];
- M_a – Anhysteretic magnetization [A/m];
- H_σ – Stress applied field [A/m];
- H_a – Applied magnetic field [A/m]: $H_a = H_s$;
- H_e – Effective field [A/m];
- H_d – Demagnetization field [A/m];
- ϕ_{mag} – Magnetic energy density;
- U_{mag} – Thermodynamic internal energy density;
- ϕ_{hys} – A separate hysteretic energy density;
- ν – Poisson's ratio;
- D_σ – Stress demagnetization term [MPa];
- Y – Young's modulus;
- σ – Applied stress [MPa];

¹L.E.B. Research Laboratory, Electrical engineering department; University of Batna, 05000 Batna, Algeria;
E-mails: mk.ykhlef@gmail.com; sebti_boukhtache@yahoo.fr; machabane@yahoo.com

- a – Effective field scaling constant [A/m];
- k – Average density of the pinning sites [A/m];
- c – Reversibility coefficient;
- α – Domain coupling constant;
- μ – Magnetic permeability [H/m];
- L – Sheet's length [mm];
- λ – Magnetostriction: $\lambda = \Delta L/L$;
- λ_s – Saturation Magnetostriction;

2 Introduction

Magneto-mechanical coupling effects can be grouped in two major phenomena. The first one is the effect of an applied stress on the magnetic behavior that often leads to significant changes of the magnetic properties. The second one is the effect of an applied magnetic field on the mechanical behavior that often leads to mechanical deformation called magnetostriction λ . The magnetostriction value ranges from about 10^{-6} to 10^{-5} [1]. This mechanical phenomenon is usually the source of noise emitted by electrical machines. Such interesting phenomenon represents the subject of recent research works [1, 2].

NO Fe-Si 3% sheets have a major importance as subject of basic research studies and industrial applications in electromagnetic devices. They have been used as the cores of electrical machines as shown by Fig. 1. Their magnetic properties are nonlinear and hysteretic. Moreover, they have a strong impact on the performance of these devices and should be carefully characterized for the evaluation and the quality control of magnetic materials.

It has been found that one of the impacts which affect the magnetic behavior of the materials is a phenomenon known as stress demagnetization [3–6]. This phenomenon leads to an internal field H_i such

$$H_i = (H_a - H_d) + (H_\sigma - D_\sigma \sigma M).$$

The term $D_\sigma = D_s \sigma$ [4] is called stress demagnetization term. The difference $(H_\sigma - D_s \sigma M)$ represents the magneto-mechanical contribution to the internal field. This term changes linearly with stress σ but sometimes it becomes negligible when tensile stress is relatively important. Thus, it produces an asymmetry in magnetic behavior under the two forms of stresses.

Several research studies are carried out in modeling the behaviors of steel sheets used in electrical machines. The most important characteristics are the magnetic hysteresis, the stress-dependency, mechanical deformation, losses, frequency and permeability.

This paper presents the basis of a new estimation model to characterize the changes in the magnetic properties due to the effect of the stress demagneti-

zation phenomenon of the ferromagnetic sheet at different loads of stresses. The new concept is based on the classic Sablik-Jiles-Atherthon model [5], which has been modified by introducing the Schneider-Cannell Watts' factor ($D_s\sigma$) in order to take into account the stress demagnetization effect. The resulting model is coupled with the Jiles dynamic model [7, 8] to include the eddy current effects [9]. On the other hand, to discuss the effect of the SDT D_s on the magnetostriction loop, the theoretical model given by Sablik [5] is used in this work. This important model is not widely used in literature because it presents difficulties related to the experimental determination of some of its parameters.

In this work, a new improved model has been developed to study the effect of stress demagnetization phenomenon on the magnetic properties of some of ferromagnetic materials under different stresses and various frequency ranges.

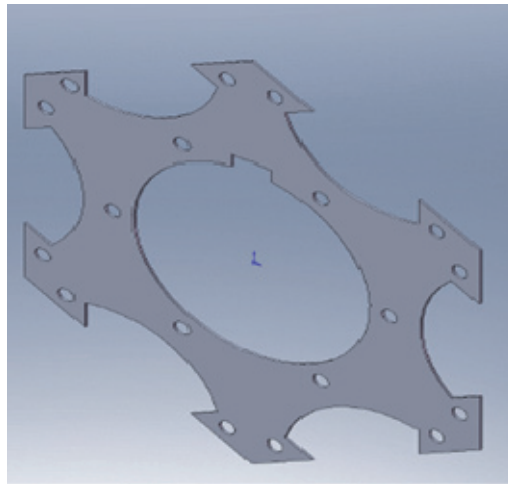


Fig. 1 – A Non-Oriented Iron-Silicon Sheet of rotor in electrical motor.

3 Description of the Models

3.1 Dynamic Model with Eddy Current Effects and Magnetization Law Model $M(H, \sigma, f)$

In the J-A model [7, 11], the total magnetization M is the sum of the reversible and the irreversible components M_{rev} and M_{irr} respectively. These components are defined by:

$$M = M_{rev} + M_{irr}, \quad (1)$$

$$M_{rev} = c(M_{an} - M_{irr}), \quad (2)$$

$$M_{irr} = M_{an} - k\delta \frac{dM_{irr}}{dH_e}, \quad (3)$$

$$M_{an} = M_s \left[\coth\left(\frac{H_e}{a}\right) - \frac{a}{H_e} \right], \quad (4)$$

The general equation for the rate of change of magnetization is given in [12] by expression (5):

$$\frac{dM}{dt} = \frac{dM}{dH} \frac{dH}{dt} + \frac{dM}{d\sigma} \frac{d\sigma}{dt}, \quad (5)$$

The magnetization M in (5) depends on both the differential susceptibility $\partial M/\partial H$ and the change in magnetization due to stress $\partial M/\partial \sigma$.

The term $\partial M/\partial \sigma$ [12] is expressed as:

$$\frac{dM}{d\sigma} = \frac{\sigma}{Y\xi} (M_{an} - M) + c \frac{dM_{an}}{d\sigma}, \quad (6)$$

The coefficient ξ , in units of energy per unit volume, governs the efficiency at which elastic energy change is converted to change in irreversible magnetization.

In equations (3) – (6), H_{is} the applied magnetic field. The parameter δ is defined to have the value (+1) when $dH/dt > 0$, and (–1) when $dH/dt < 0$.

To consider the dynamic state and extend the use of this model to high frequencies, eddy current effects must be included in the magnetization model at fixed temperature.

In the previous work [9], the model of $\partial M/\partial H$ has been developed in details, in which the parameters K_1 and K_2 are considered. These parameters represent the coefficients related to anomalous loss and classical eddy current losses respectively, where:

$$K_1 = \left(\frac{Gd_1 w H_0 \mu_0}{\rho} \right)^{\frac{1}{2}}, \quad K_2 = \frac{\mu_0^2 d_1^2}{2\rho\beta},$$

d_1 is the plate thickness of the sheet, ρ is the resistivity, β is a geometry factor, $G = 0.1356$ [13, 14] is a dimensionless constant, w is the plate width and H_0 represents the fluctuating internal field experienced by the domain walls [9].

In this paper, the model of $\partial M/\partial H$ is modified by introducing the effect of the stress demagnetization term expressed in term of $\alpha_e(\sigma)$. This latter quantifies the amount of domain interaction under application of external stress and will be detailed in Subsection 3.2.

The $\partial M/\partial H$ model to be resolved is given as follows:

$$\left(k\delta - \alpha_e(\sigma) \left(M_{an} - M + k\delta c \frac{dM_{an}}{dH_e} \right) \right) \frac{dM}{dH} - \left(M_{an} - M + k\delta c \frac{dM_{an}}{dH_e} \right) + K_2 \frac{dH}{dt} \left(\frac{dM}{dH} \right)^2 + K_1 \left(\frac{dH}{dt} \right)^{1/2} \left(\frac{dM}{dH} \right)^{3/2} = 0, \quad (7)$$

Model (7) describes the hysteresis law $M(H, \sigma, f)$ as a function of $\alpha_e(\sigma)$ and the frequency f .

3.2 Magnetostriction law model $\lambda(M)$

The magneto-mechanical model of Sablik-Jiles-Atherton [12] is modified by introducing the demagnetization field H_d and the term $D_\sigma M$ [3]. So, the effective field H_e becomes equal to:

$$H_e = H_a - H_d + \alpha M - D_\sigma M + H_\sigma, \quad (8)$$

where, H_σ is known as the stress effective field and is proportional to stress. In this paper, the stress axis is assumed to be aligned with the field direction as shown by Fig. 2.

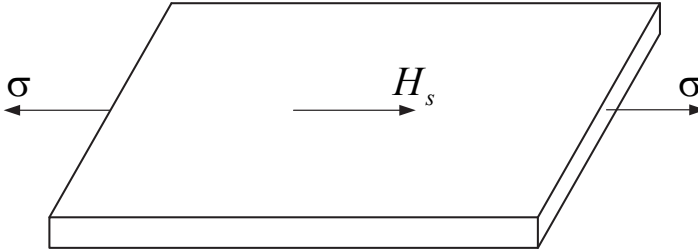


Fig. 2 – A Non-Oriented Iron-Silicon Sheet Geometry under uniaxial stress (with 0.5 mm thickness).

The stress effective field is thus proportional to the magnetization derivative of the bulk magnetostriction and is given by:

$$H_\sigma = \frac{3\sigma}{2\mu_0} \frac{d\lambda}{dM}, \quad (9)$$

The quantity λ refers to the bulk magnetostriction.

By introducing (9) into (8) yields to (10):

$$H_e = H + (\alpha - D_\sigma)M + \frac{3\sigma}{2\mu_0} \frac{d\lambda}{dM_a}, \quad (10)$$

where $H = H_a - H_d$.

The differentiation of (10) gives:

$$\frac{dH_e}{dH} = 1 + \left(\alpha - D_\sigma + \frac{3\sigma}{2\mu_0} \frac{d^2\lambda}{dM_a^2} \right) \frac{dM}{dH}, \quad (11)$$

$$\frac{dH_e}{dH} = 1 + \alpha_e(\sigma) \frac{dM}{dH}, \quad (12)$$

So:

$$\alpha_e(\sigma) = \left(\alpha - D_\sigma + \frac{3\sigma}{2\mu_0} \frac{d^2\lambda}{dM_a^2} \right), \quad (13)$$

D_σ is defined in [4] as:

$$D_\sigma = \frac{3\lambda_s}{\mu_0 M_s^2} \sigma = D_s \sigma, \quad (14)$$

Therefore, $D_s = \frac{3\lambda_s}{\mu_0 M_s^2}$.

By substituting (14) in (13) yields to (15):

$$\alpha_e(\sigma) = \left[\alpha - \left(\frac{3\lambda_s}{\mu_0 M_s^2} + \frac{3}{2\mu_0} \frac{d^2\lambda}{dM_a^2} \right) \sigma \right], \quad (15)$$

In order to study the influence of the applied magnetic field H on the mechanical behavior of the alloy while taking into account the stress demagnetization effect, the model proposed by Sablik in [5] is used:

$$\lambda = -\left(\frac{b(1+\nu)}{Y}\right) \cdot \left\{ \left\{ 1 + \left(\frac{9Y}{2b^2(1+\nu)^2}\right) \varphi_{mag}(M_s) \right\}^{\frac{1}{2}} - \left\{ 1 + \frac{9Y}{2b^2(1+\nu)^2} (\varphi_{mag}(M_s) - \varphi_{mag}(M)) \right\}^{\frac{1}{2}} \right\}, \quad (16)$$

with: $\varphi_{mag} = U_{mag} + \varphi_{hys}$,

$$U_{mag} = \frac{1}{2} \hat{\alpha} \mu_0 M^2, \quad (17)$$

$$\varphi_{hys} = \frac{1}{2} \alpha'' \mu_0 (M_a - M)^2 - \alpha' \mu_0 (M_a - M) H,$$

$\hat{\alpha}$ is the domain coupling constant.

The main drawback of Sablik's model is the determination of the parameters α' and α'' . These parameters are experimental hysteretic terms which describe the cycling behavior of magnetostriction loop λ . In the present paper, the specimen used is a polycrystalline ferromagnetic which has the same characteristics than the one studied by Sablik in [5]. Therefore, the values of α' and α'' are exploited in this work, where is $\alpha' = 7.5 \times 10^6$ and $\alpha'' = 3.5 \times 10^5$.

For the isotropic case [5]: $\nu = c_{12} / (c_{11} + c_{12})$, $Y = c_{11} - 2c_{12} \nu$, then:

$$c_{44} = (c_{11} - c_{12}) / 2, \quad (18)$$

c_{11} , c_{12} and c_{44} represent the elastic coefficients [kN/m²].

The derivative of the magnetostriction with respect to the magnetization $d\lambda/dM_a$ in the anhysteretic state [5] is given by:

$$\frac{d\lambda}{dM_a} = \frac{-(7/2)(|b|/b)(\lambda_s/M_s)M}{\left[M_s^2 + (21/4)(M_s^2 - M^2)\right]^{1/2}}, \quad (19).$$

where, the magneto-elastic coupling constant b [kN/m²] is defined as:

$$b = [(2/5)\lambda_{100} + (3/5)\lambda_{111}]c_{44}, \quad (20)$$

The saturation magnetostriction λ_s is related to the constant b as:

$$\lambda_s = [(-2/3)b(1 + \nu)] / Y, \quad (21)$$

The coefficient λ_{100} is the saturation magnetostriction with the magnetic moments aligned along the [100] axis, and λ_{111} corresponds to the case of magnetic moments aligned along the [111] axis. Elastic and magnetostrictive parameters are given in **Table 1**.

Table 1

Elastic and magnetostrictive coefficients of the ferromagnetic sheet.

	c_{11} [GPa]	c_{12} [GPa]	λ_{100}	λ_{111}
NO Fe-Si 3%	202	122	$23 \cdot 10^{-6}$	$-4.5 \cdot 10^{-6}$

The coefficient α in equation (15) is replaced by $\hat{\alpha}$ which is related to the saturation magnetostriction λ_s [5] as:

$$\hat{\alpha} = (21/4) \frac{Y}{\mu_0} \left(\frac{\lambda_s}{M_s} \right)^2, \quad (22)$$

$$\alpha_e(\sigma) = \left[\hat{\alpha} - \left(\frac{3\lambda_s}{\mu_0 M_s^2} + \frac{3}{2\mu_0} \frac{d^2 \lambda}{dM_a^2} \right) \sigma \right], \quad (23)$$

By substituting (22) into (23) yields:

$$\alpha_e(\sigma) = \frac{1}{2} \frac{3\lambda_s}{\mu_0 M_s^2} \left[\frac{7Y\lambda_s}{2} - \left(\frac{M_s^2}{\lambda_s} \frac{d^2 \lambda}{dM_a^2} + 2 \right) \sigma \right], \quad (24)$$

Finally,

$$\alpha_e(\sigma) = \frac{D_s}{2} \left[\frac{7Y\lambda_s}{2} - \left(\frac{M_s^2}{\lambda_s} \frac{d^2 \lambda}{dM_a^2} + 2 \right) \sigma \right], \quad (25)$$

Equation (25) demonstrates that the new expression of $\alpha_e(\sigma)$ is a function of the stress σ .

3.3 Results of parameters fitting

The model parameters $k, \bar{\alpha}, c, a$ in (17) are first obtained from the parameters calculation algorithm by using the measured properties. This gives a first approximation based only on four particular points on the curve [15]. Then, the parameters have been optimized by using an iterative method combined with the Regula-falsi algorithm to obtain a better fit over the entire range of the measured hysteretic loop. The initial data have been extracted from the previous work [9]. The optimized parameters are represented in **Table 2**.

Table 2
Model estimated parameters for NO Fe-Si 3% steel.

	k [A/m]	$\bar{\alpha}$	a [A/m]	c
Initial parameters	58.855	$1.69 \cdot 10^{-4}$	130.22	0.00854
Optimised parameters	58.5334	$1.75 \cdot 10^{-4}$	129.8597	0.0061

4 Modeling and Results

4.1 Magnetic hysteresis

The estimated model is obtained from combination of (7), (16), (17) and (25). It is applied to examine the stress demagnetization effect on the magnetic and mechanical behaviors in the electrical sheet (NO Fe-Si 3%) with 0.5 mm thick, under sinusoidal field with $H_{\max} = 1000$ A/m. The saturation magnetization $M_s = 1.61 \cdot 10^{+6}$ A/m and quasi-static frequency equal to 1 Hz. The simulation has been carried out using Matlab software. It is important to mention here that (7) is available for both dynamic and quasi-static cases. However, in order to simplify the study and to model separately the effect of the physical parameter D_σ from the frequencies effects, only quasi-static case has been analyzed.

Fig. 3 shows the effect of stress when the physical factor D_σ is not included in the model. The influence of tensile stress ($\sigma > 0$) is to displace the hysteresis loop upper than the one plotted when the stress σ is removed. Thus the slope of the hysteresis loop, the coercive H_C , the hysteresis losses W_{hys} ($W_{hys} = \int B dH$) and the remanent magnetization M_r increases, but the susceptibility χ_{max} decreases. Under compressive stress ($\sigma < 0$), the displacement of hysteretic loop is lower than the one without stress. Thus the slope and all the magnetic parameters cited above decrease.

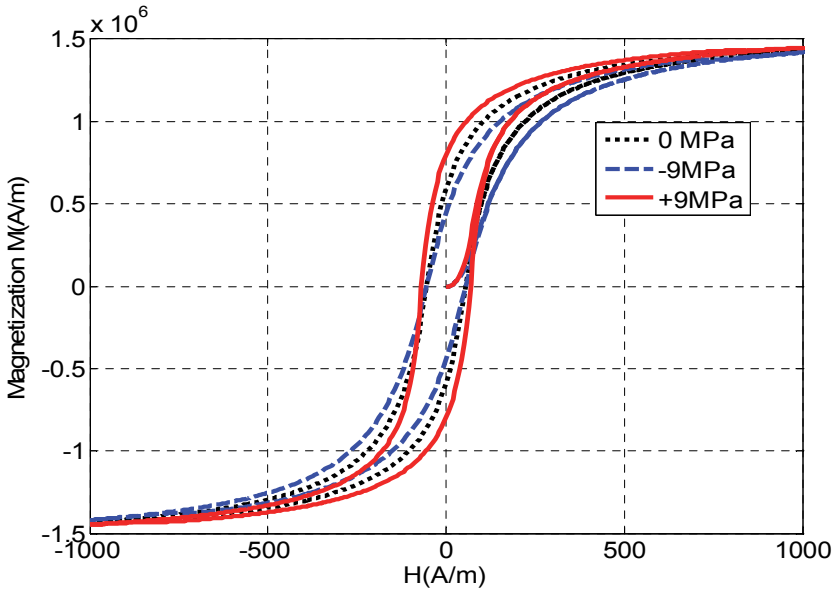


Fig. 3 – First magnetization and hysteresis curve for a Non-Oriented Iron-Silicon. Effect of external stress without including the SDT D_σ .

Simulation results presented in Fig. 4 are obtained by introducing the physical parameter D_σ in the model. Fig. 4a shows clearly the effect of the SDT D_σ on the magnetic properties of the alloy. The effect of tensile stress is to displace the hysteresis loop lower than the one plotted when the stress σ is removed. In fact, the slope of the hysteresis loop, the remanent magnetization M_r and the susceptibility χ_{max} decrease, but the coercive H_C and the hysteresis losses increase. The inverse effect is seen when compressive stress is applied. In fact, the displacement of hysteresis loop is higher than the loop plotted when the stress is removed. Thus the slope of the hysteresis loop, the coercive H_C , the hysteretic losses and the magnetization M_r increase. These results evolve in the same manner as those presented by Sablik in [3, 5] for polycrystalline steel

other than the NO Fe-Si 3%. The changes in the magnetic properties of the sheet for the two cases are presented in **Table 3**.

Table 3
Parameter D_σ Effect's on the Magnetic Properties of a NO Fe-Si 3%.

σ [MPa]	$\sigma = +9$		$\sigma = 0$	$\sigma = -9$	
	$D_\sigma \neq 0$	$D_\sigma = 0$	-	$D_\sigma \neq 0$	$D_\sigma = 0$
H_C [A/m]	63.952	68.7432	54.4854	55.1957	54.6273
M_r [A/m]	$5.7273 \cdot 10^5$	$7.9775 \cdot 10^5$	$5.8919 \cdot 10^5$	$6.4165 \cdot 10^5$	$4.448 \cdot 10^5$
W_{hys} [kJ/m ³]	726.8958	774.4237	369.0852	743.6787	695.9880
χ_{max} [Wb/Am]	$1.0952 \cdot 10^4$	$2.4395 \cdot 10^4$	$1.3902 \cdot 10^4$	$1.7212 \cdot 10^4$	$0.8889 \cdot 10^4$

4.2 Discussion

The expression $H_e = H + \alpha M + H_\sigma$ does not exhibit an asymmetry in the behaviour of magnetic properties under tension and compression. But, the use of (8) leads to the results presented in **Table 3**, where, it is clearly seen an asymmetry on magnetic properties corresponding to two cases.

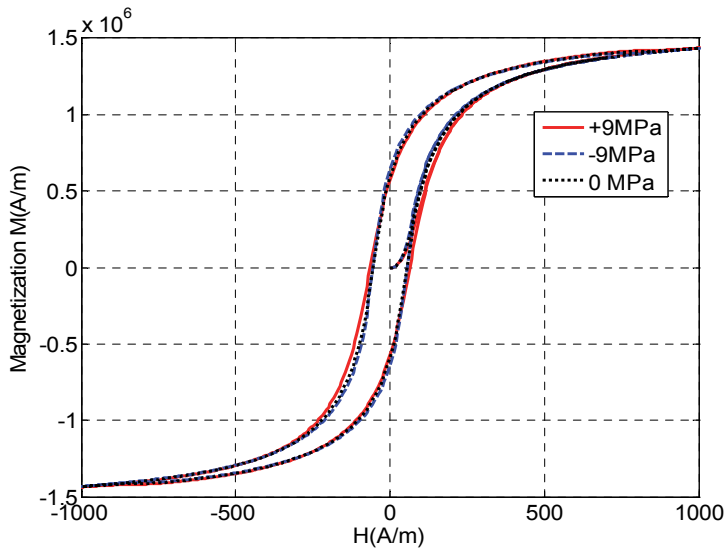


Fig. 4a – First magnetization and hysteresis curve for Non-Oriented Iron-Silicon, SDT D_σ is included.

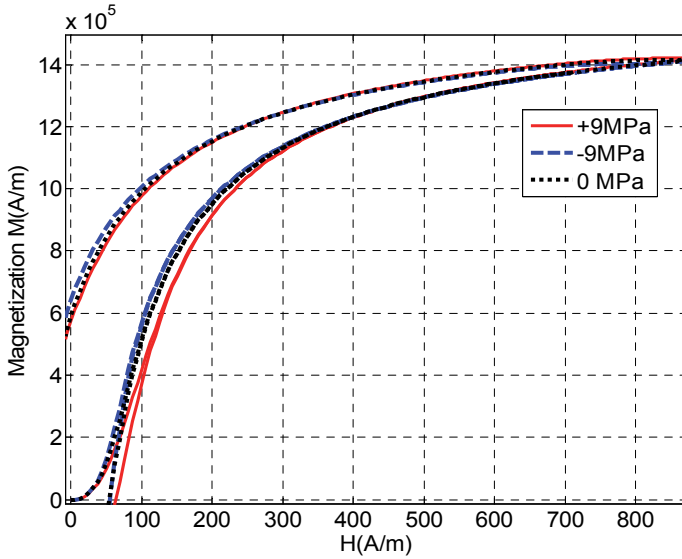


Fig. 4b – Variation in remanent magnetization M_r .

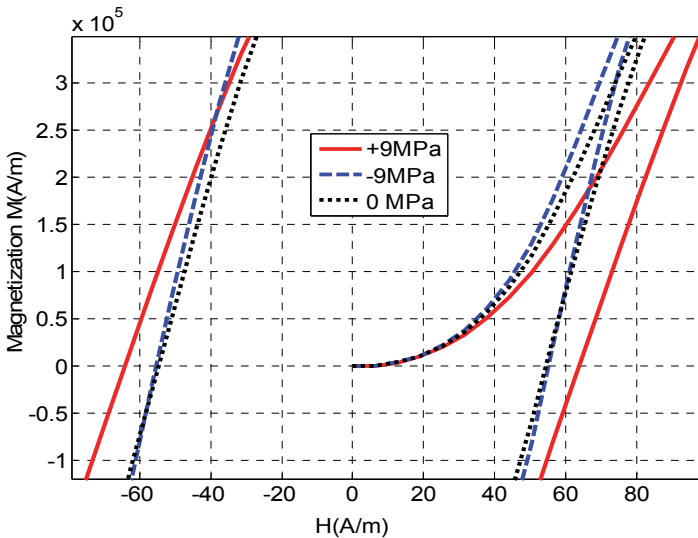


Fig. 4c – Variation in coercive field H_c .

The first case is when the term D_σ is introduced in the model and the second one is when the SDT D_σ is neglected. This asymmetry is observed on the coercive field H_c , the magnetization M_r , the hysteretic losses W_{hys} and the susceptibility χ_{max} . This phenomenon is caused by the presence of many dislocations which are produced under applied magnetic field and stress. There

are some internal deformations related to both the demagnetization field effect ($-H_d$) and the effect of the term ($D_s M \sigma$). These physical parameters act in opposition for a compressive stress, whereas they act in coordination for a tensile stress.

4.3 Magnetostriction loops

Figs. 5a and 5b show the magnetostrictive behavior of the NO Fe-Si 3% under external stresses. The plotted curves obtained by applying the model $\lambda(H)$ given by (16). The curves start from zero associated to the absence of both magnetic field and stress.

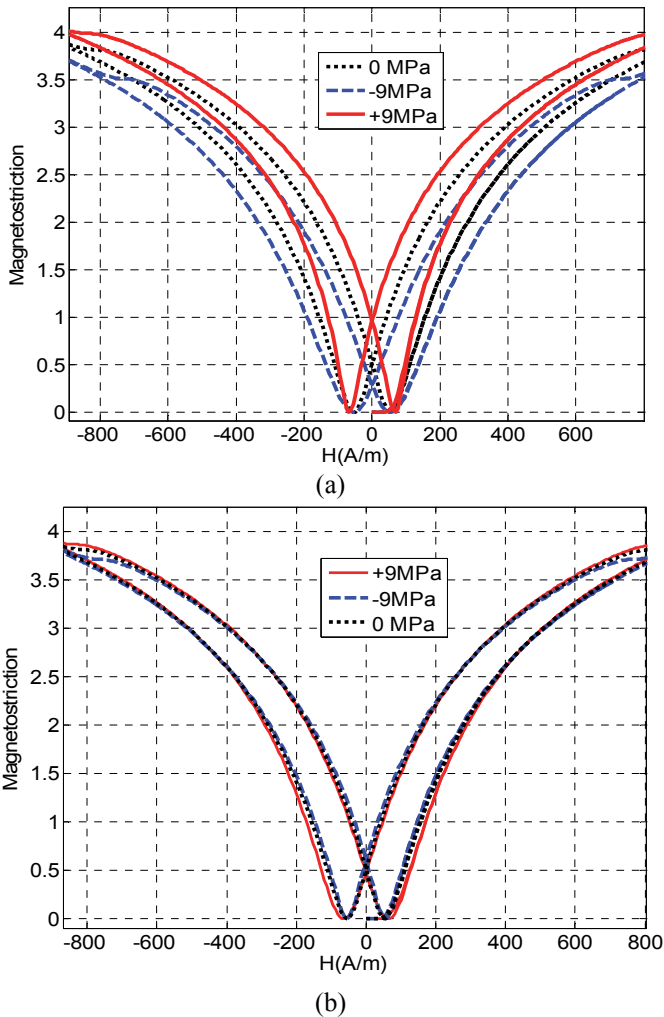


Fig. 5 – First Magnetostriction and Magnetostriction loop for a Non-Oriented Iron-Silicon: (a) SDT D_σ is not included, (b) SDT D_σ is included.

Fig. 5a shows the results when the physical parameter D_σ is not included in the model. Referring to this case, it is clearly shown that the tensile stress tends to increase the magnetostriction amplitude and the compressive stress tends to decrease it with respect to the loop without stress σ . Such an important variation between the curves is remarked.

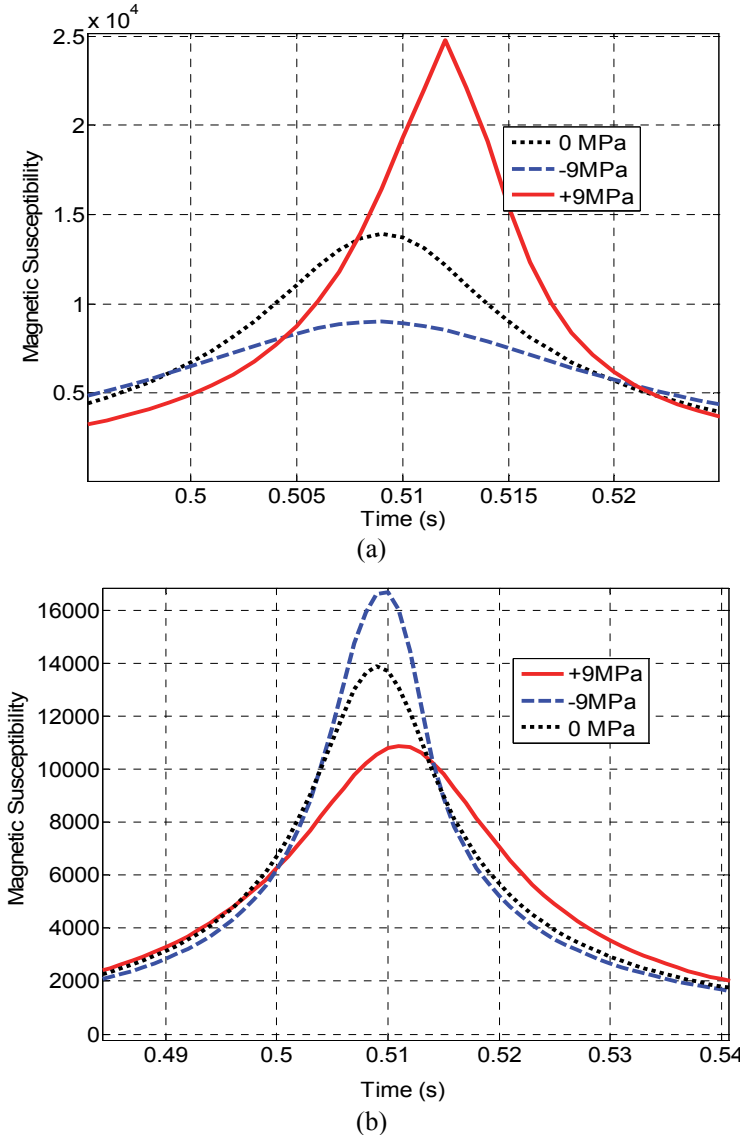


Fig. 6 – Secant magnetic susceptibility for a Non-Oriented Iron-Silicon.
 (a) SDT D_σ is not included, (b) SDT D_σ is included.

Results shown in Fig. 5b have been obtained when the SDT D_σ is taking in to account. It is found that this parameter improves clearly the results under both compressive and tensile stresses. The three magnetostrictive loops are very close to each other.

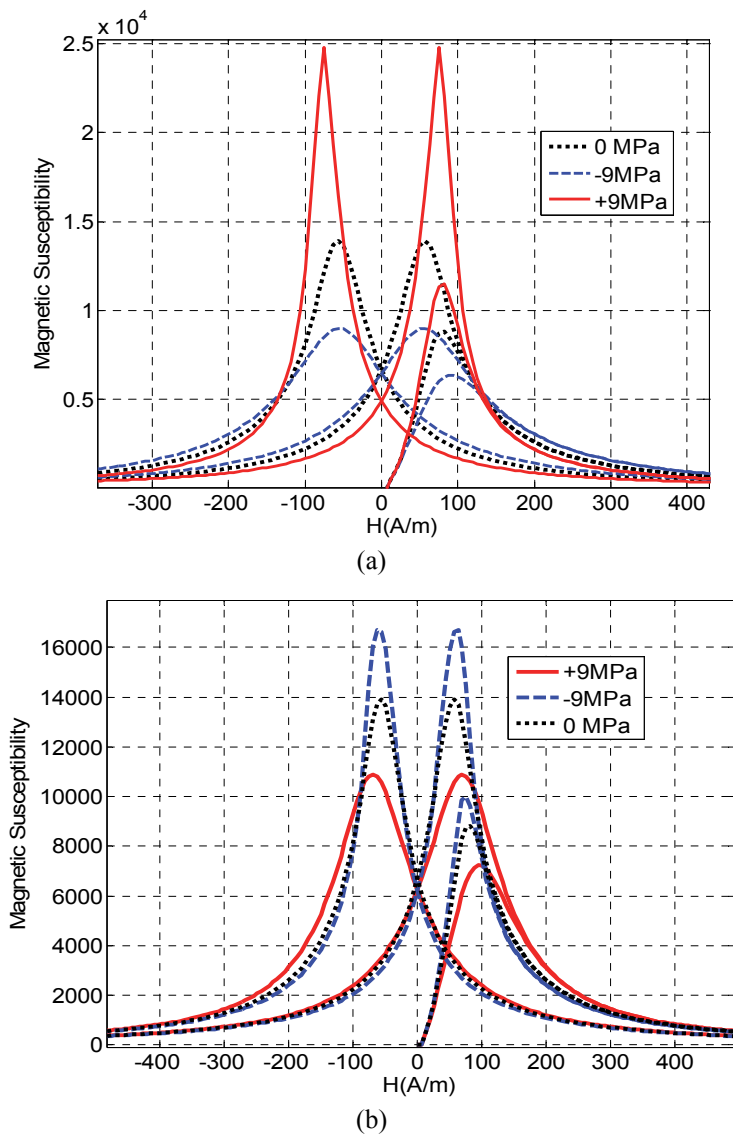


Fig. 7 – Magnetic susceptibility for a Non-Oriented Iron-Silicon under stresses: (a) SDT D_σ is not included, (b) SDT D_σ is included.

Another way to study the effect of the parameter D_σ on the magnetic behavior of the alloy is to plot the magnetic differential susceptibility dM/dH as a function of time as presented in Figs. 6a and 6b, then as a function of the field intensity as illustrated in Figs. 7a and 7b. The curves in the last case start from zero.

When the SDT D_σ is neglected, an important decrease is seen in the susceptibilities $\chi_{\max}(t)$ and $\chi_{\max}(H)$ under tensile stress. But, a large increase is observed under compressive stress as shown by Figs. 6a and 7a. When the SDT D_σ is included the effect is opposite. In fact, a relative improvement in the susceptibilities $\chi_{\max}(t)$ and $\chi_{\max}(H)$ is observed respectively, under compressive and tensile stresses with respect to curves without stress as shown by Figs. 6b and 7b.

5 Conclusion

In the present paper, we have interested to introduce in Sablik-Jiles-Atherton model the eddy current effects and the physical parameter D_σ which is often negligible in literature. In order to model separately the physical parameter D_σ effect from the eddy current effects, the work presented here is restricted to low frequencies. The influence of the parameter D_σ on the magnetic behavior $M(H, \sigma, f)$ and the magnetostrictive behavior $\lambda(H)$ has been discussed by applying of the proposed model on a NO Fe-Si 3% sheet under uniaxial and external stresses.

The presented results show clearly that the magnetic properties depend strongly on the physical parameter D_σ that lead to an asymmetry on both magnetic and magnetostrictive behaviors of the alloy under the two forms of stresses.

Based on the study carried out by the present work, it has been confirmed that the stress demagnetization parameter D_σ need to be taken into account in order to ensure a full and an accurate characterization of the alloy which is subject to stresses. Recommendations are made for further research work by considering both the characteristic parameter D_σ and various frequency ranges.

6 References

- [1] L. Daniel: Multiscale Modeling of the Magneto-mechanical behaviour of Textured Ferromagnetic Materials, PhD Thesis, Paris University, France, 2003. (In French).
- [2] L. Daniel, M. Rekik, O. Hubert: A Multiscale Model for Magneto-Elastic Behavior Including Hysteresis Effects, Archive Applied Mechanics, Vol. 84, No. 9-11, Oct. 2014, pp. 1307 – 1323.
- [3] M.J. Sablik: A Model for Asymmetry in Magnetic Property Behavior under Tensile and Compressive Stress in Steel, IEEE Transaction on Magnetics, Vol. 33, No. 5, Sept. 1997, pp. 3958 – 3960.

- [4] C.S. Schneider, P.Y. Cannell, K.T. Watts: Magneto-Elasticity for Large Stresses, IEEE Transaction on Magnetics, Vol. 28, No. 5, Sept. 1992, pp. 2626 – 2631.
- [5] M.J. Sablik, D.C. Jiles: Coupled Magnetoelastic Theory of Magnetic and Magnetostrictive Hysteresis, IEEE Transaction on Magnetics, Vol. 29, No. 4, July 1993, pp. 2113 – 2123.
- [6] M.J. Sablik, L.A. Riley, G.L. Burkhardt, H. Kwun, P. Y. Cannell, K.T. Watts, R.A. Langman: Micromagnetic Model for Biaxial Stress Effects on Magnetic Properties, Journal of Magnetism and Magnetic Materials, Vol. 132, No. 1-3, April 1994, pp. 131 – 148.
- [7] D.C. Jiles: Modeling the Effects of Eddy Current Losses on Frequency Dependent Hysteresis in Electrically Conducting Media, IEEE Transaction on Magnetics, Vol. 30, No. 6, Nov. 1994, pp. 4326 – 4328,
- [8] D.C. Jiles: Frequency Dependence of Hysteresis Curves in Conducting Magnetic Materials, Journal of Applied Physics, Vol. 76, No. 10, 1994, pp. 5849 – 5855.
- [9] S. Boukhtache, M. Yakhlef, M. Chabane: Magnetic Field Computation in a Non-oriented Sheet Cross-section Considering the Hysteresis Phenomenon, Journal of Magnetism and Magnetic Materials, Vol. 322, No. 5, March 2010, pp. 505 – 509.
- [10] V. Maurel: Influence of Multiaxial Mechanical Condition Induced by Cutting on Magnetic Steel Sheet Properties, PhD Thesis, Paris University, France, 2002. (In French).
- [11] D.C. Jiles, D.L. Atherton: Theory of Ferromagnetic Hysteresis, Journal of Magnetism and Magnetic Materials, Vol. 61, No. 1-2, Sept. 1986, pp. 48 – 60.
- [12] D.C. Jiles: Theory of the Magnetomechanical Effect, Journal of Physics D: Applied Physics, Vol. 28, No. 8, 1995, pp. 1537 – 1546.
- [13] G. Bertotti: General Properties of Power Losses in Soft Ferromagnetic Materials, IEEE Transaction on Magnetics, Vol. 24, No. 1, Jan. 1988, pp. 621 – 630.
- [14] G. Bertotti: Some Considerations on the Physical Interpretation of Eddy Current Losses in Ferromagnetic Materials, Journal of Magnetism and Magnetic Materials, Vol. 54-57, No. 3, Feb. 1986, pp. 1556 – 1560.
- [15] D.C. Jiles, B. Thielke, M.K. Devine: Numerical Determination of Hysteresis Parameters for the Modeling of Magnetic Properties using the Theory of Ferromagnetic Hysteresis, IEEE Transaction on Magnetics, Vol. 28, No.1, Jan. 1992, pp. 27 – 35.
- [16] M.J. Sablik, D.C. Jiles: A Model for Hysteresis in Magnetostriction, Journal of Applied Physics, Vol. 64, No. 10, Nov. 1988. pp. 5402 – 5404.